COMPUTER RESEARCH AND MODELING
2024 VOL. 16 NO. 4 P. 913–925
DOI: 10.20537/2076-7633-2024-16-4-913-925

Ки&М

MODELS IN PHYSICS AND TECHNOLOGY

UDC: 532.685

Simulation of two-phase flow in porous media using an inhomogeneous network model

K. Shabbir[1,a], O. Ya. Izvekov[1,b], A. V. Konyukhov[1,2,c]

[1]Moscow Institute of Physics and Technology,
9 Institutsky lane, Dolgoprudny, Moscow region, 141700, Russia
[2]Joint Institute for High Temperatures of the Russian Academy of Sciences,
13/2 Izhorskaya st., Moscow, 125412, Russia

E-mail: [a] kafiulshabbir@phystech.edu, [b] izvekov_o@inbox.ru, [c] konyukhov_av@mail.ru

Received 17.10.2023, after completion — 20.05.2024.
Accepted for publication 13.06.2024.

We present an inhomogeneous two-dimensional network model of two-phase flow in porous media. The edges of the network are assumed to be capillary tubes of different radii. We propose a new algorithm for handling phase fluxes at the nodes of this network model. We perform two test problems and show that the two-phase flow in this inhomogeneous network model demonstrates properties that are analogous to those of real porous media: capillary imbibition, dependence of capillary pressure on saturation and effect of capillary forces in two-phase displacement. The two test problems are: the counter-current imbibition and the two-phase displacement in a periodically inhomogeneous porous medium. In the former problem, we implement a network consisting of two regions: a region of low-permeability with thin capillaries surrounded by a region of high-permeability with thick capillaries, initially saturated with wetting and nonwetting incompressible fluids, respectively. Capillary equilibrium is established due to counter-current imbibition by a region. We examine the dependence: of saturation of the wetting fluid with respect to time in the regions, and of capillary pressure on the current saturation. We have obtained a qualitative agreement with the known experimental and theoretical results, which will further allow us to use this network model to verify homogenized models of capillary nonequilibrium. In the latter problem, we consider the two-phase displacement, where the network is initially saturated with non-wetting fluid. Then wetting fluid is injected through a boundary at a constant rate. We analyze the saturation with respect to the axis which is along the applied pressure gradient for various moments in time with various values of coefficients of surface tension. The results show that for lower values of coefficient of surface tension, the wetting fluid prefers to invade through the thicker tubes, and in the case of higher values, through thinner tubes.

Keywords: porous medium, capillary pressure, imbibition, multiphase flow, network model, periodically inhomogeneous media

Citation: *Computer Research and Modeling*, 2024, vol. 16, no. 4, pp. 913–925.

The project was supported by the Russian Science Foundation, grant No. 23-21-00175 (https://rscf.ru/project/23-21-00175/).

КОМПЬЮТЕРНЫЕ ИССЛЕДОВАНИЯ
И МОДЕЛИРОВАНИЕ 2024 Т. 16 № 4 С. 913–925
DOI: 10.20537/2076-7633-2024-16-4-913-925

Ки&М

МОДЕЛИ В ФИЗИКЕ И ТЕХНОЛОГИИ

УДК: 532.685

Моделирование двухфазного течения в пористых средах с использованием неоднородной сетевой модели

К. Шаббир[1,a], О. Я. Извеков[1,b], А. В. Конюхов[1,2,c]

[1]Московский физико-технический институт,
Россия, 141700, Московская область, г. Долгопрудный, Институтский переулок, д. 9
[2]Объединенный институт высоких температур РАН,
Россия, 125412, г. Москва, ул. Ижорская, д. 13, стр. 2

E-mail: [a] kafiulshabbir@phystech.edu, [b] izvekov_o@inbox.ru, [c] konyukhov_av@mail.ru

Получено 17.10.2023, после доработки — 20.05.2024.
Принято к публикации 13.06.2024.

Представлена неоднородная двумерная сетевая модель двухфазного течения в пористых средах. Предполагается, что ребра сети представляют собой капиллярные трубки разного радиуса. Предложен новый алгоритм управления фазовыми потоками в узлах этой сетевой модели. Показано, что сетевая модель демонстрирует свойства, аналогичные свойствам реальных пористых сред: капиллярная пропитка, зависимость капиллярного давления от насыщенности и влияние капиллярных сил при двухфазном течении. Было решено две тестовые задачи: противоточная пропитка пористого блока и двухфазное течение в периодически неоднородной пористой среде. В первой задаче реализована сеть, состоящая из двух областей: область с низкой проницаемостью и тонкими капиллярами окружена областью с высокой проницаемостью и толстыми капиллярами, изначально насыщенными смачивающими и несмачивающими несжимаемыми жидкостями соответственно. Капиллярное равновесие устанавливается за счет противоточной пропитки внутренней области. Исследована зависимость насыщенности смачивающей жидкости в областях от времени и капиллярного давления от текущей насыщенности. Получено качественное соответствие известным экспериментальным и теоретическим результатам, что в дальнейшем позволит использовать эту сетевую модель для проверки осредненных моделей капиллярной неравновесности. Во второй задаче рассматривается двухфазное вытеснение, при котором сеть изначально насыщается несмачивающей жидкостью. Затем смачивающая жидкость вводится через границу с постоянным расходом. Анализируется распределение насыщенности вдоль оси, направленной вдоль приложенного градиента давления, для различных моментов времени при различных значениях коэффициентов поверхностного натяжения. Результаты расчетов показывают, что при более низких значениях коэффициента поверхностного натяжения смачивающая жидкость предпочитает проникать через более толстые трубки, а при более высоких значениях — через более тонкие.

Ключевые слова: пористая среда, капиллярное давление, пропитка, многофазный поток, сетевые модели, периодически неоднородные среды

Проект поддержан Российским научным фондом, грант № 23-21-00175 (https://rscf.ru/project/23-21-00175/).

1. Introduction

Modeling two-phase flow in porous media is important in a variety of applications in oil production, hydrology, etc [Labed, Bennamoun, Fohr, 2012]. A porous medium consists of a skeleton (usually solid) and voids (also called pores). The voids are connected to each other by capillaries. The voids may contain fluids such as water, oil or gas [Su, Sanchez, Yang, 2012]. The saturation S_k of fluid F_k is defined as the ratio of the volume V_k occupied by the fluid F_k to the total volume of the void space V_{void}:

$$S_k = \frac{V_k}{V_{\text{void}}}. \tag{1}$$

We assume that the void space can be filled with only two fluids. We denote saturation with a more wetting fluid (for example, water in a hydrophilic rock) as S_w, and with a less wetting fluid (for example, oil in a hydrophilic rock) as S_{nw}. Let these fluids completely fill the space of pores and capillaries, then $S_w + S_{nw} = 1$. In what follows, we denote the saturation of the wetting fluid as S. Darcy's law is a continuum law for linear filtration of fluids in a porous medium [Whitaker, 1986]:

$$Q = -\frac{K}{\mu}\nabla P, \tag{2}$$

where Q is the flow rate, K is the permeability, μ is the coefficient of viscosity, and ∇P is the pressure gradient.

Permeability in the case of multiphase flows is traditionally considered to be a function of saturation $K = K(S)$ [Coussy, 2004].

However, this assumption is only valid when the characteristic time of the fluid flow is much greater than the characteristic time of relaxation, which is the time required for redistribution of fluids in the pore and capillary space due to surface tension forces. Here, it is also assumed that the fluid configuration corresponds to minimum surface energy at every moment in time. Thus, the traditional models of fluid filtration in a porous medium are also called equilibrium models. The capillary equilibrium can be disturbed when the saturation changes relatively quickly or the relaxation time to the equilibrium state is sufficiently long. For example, the relaxation time is long for the continuum description of filtration in a fractured-porous medium [Barenblatt, Zheltov, Kochina, 1960; Barenblatt, Patzek, Silin, 2003]. In these cases the assumption that permeability is a function of saturation is insufficient. Advanced models such as [Hassanizadeh, Gray, 1987] and [Hassanizadeh, 2004] take capillary nonequilibrium effects (dynamic effects) into account by having K to also be dependent on the rate of change of saturation:

$$K = K\left(S, \frac{\partial S}{\partial t}\right). \tag{3}$$

However, the process of fluid redistribution in the pore space can occur even at a constant saturation $S = \text{const}$. This fact can be taken into account by including an internal parameter ξ in the arguments of K. The relative permeability is of the form

$$K_\alpha = K_\alpha(S, \xi), \tag{4}$$

and the kinetic equation for the parameter ξ, such that it relaxes to an equilibrium value for a given constant saturation S:

$$\frac{\partial \xi}{\partial t} = \Omega(S, \xi). \tag{5}$$

This approach was implemented by Kondaurov in his works [Kondaurov, 2007; Kondaurov, 2009]. Equations of the form (5) have been developed by [Konyukhov, Pankratov, Voloshin, 2017; Konyukhov, Pankratov, Voloshin, 2019].

In order to better understand the physical meaning of nonequilibrium models and to clarify the parameters included in them it is necessary to consider the movement of fluids at the scale of pores

and capillaries. Common methods for modeling the movement of fluids at the pore scale are: the lattice Boltzmann method [Chen, Doolen, 1998], a direct solution of the Navier – Stokes equation, and network models [Blunt et al., 2013]. Direct modeling gives fairly accurate results on the distribution of velocity, pressure and positions of interfaces but it requires significant computing power and time [Liu et al., 2013]. Network models [Fatt, 1956; Aker et al., 1998; Ramstad, Berg, Thompson, 2019; Shabbir, 2023] allows us to qualitatively reproduce the observed effects with lower computational effort [Meakin, Tartakovsky, 2009]. This paper presents a two-dimensional network model that allows us to reproduce nonequilibrium phenomena during two-phase flow in a porous medium.

2. Numerical model of two-phase flow of incompressible fluids

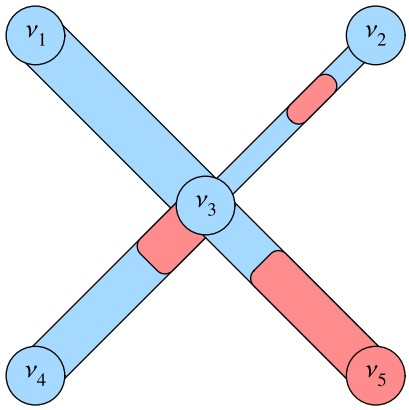

Figure 1. Scheme of the network model. Showing nodes $\{\nu_k\}$, where $k = (1, 2, 3, 4, 5)$. Each tube connecting 2 nodes ν_i and ν_j, can have a different radius R_{ij}, and contain a maximum of 2 menisci

We consider a network model of a porous medium, which is a set of nodes connected to each other by capillary tubes. The tubes model the capillary space, and the nodes model the pore space. Each node is connected to 4 neighboring nodes as shown in Fig. 1. A node can be connected to less than 4 nodes if they are located on the boundaries. In what follows, the double index ij denotes quantities related to the capillary τ_{ij} connecting nodes ν_i and ν_j of the set of nodes $\{\nu_k\}$, $k = 1, \ldots, n$, here n is the total number of nodes in the system. Capillary tubes are considered to be cylinders of circular cross-section and in general have different radii R_{ij} [Shabbir, 2023]. The medium is saturated with two incompressible fluids F_1 and F_2, with different viscosities μ_1 and μ_2, and wetting properties. The volumes of the nodes are neglected. The distribution of fluids in the medium is determined by the position of the menisci. In the model under consideration the number of menisci in one tube does not exceed 2. This model has many characteristics similar to [Aker et al., 1998], however, it is different for example, about the choice of geometry of the capillary, they have used hourglass shaped tubes, while we have used cylindrical shaped tubes, which allows us to derive accurate flow rate equations. The volumetric flow rate for a tube τ_{ij} is

$$Q_{ij} = A_{ij}\Delta P_{ij} + B_{ij}, \tag{6}$$

where the pressure difference at the ends of the tube is equal to $\Delta P_{ij} = P_i - P_j$,

$$A_{ij} = \frac{\pi R_{ij}^4}{8M_{ij}l}, \tag{7}$$

$$B_{ij} = \frac{\pi R_{ij}^4}{8M_{ij}l}\frac{2s_{ij}\sigma}{R_{ij}}, \tag{8}$$

where l is the length of the tube, σ is the coefficient of surface tension, $M_{ij} = \frac{(\mu_1 l_1 + \mu_2 l_2)_{ij}}{l}$ is the average viscosity of the fluid in the capillary τ_{ij}, μ_k is the coefficient of dynamic viscosity of the fluid F_k, and $(l_k)_{ij}$ is the length occupied by the fluid F_k in the capillary τ_{ij} ($k = 1, 2$). The multiplier s_{ij} takes into account the number and orientation of menisci in the capillary τ_{ij}, when calculating the total capillary pressure jump in the tube. The multiplier $s_{ij} = 0$ if the ends of the tube are filled with identical fluids, $s_{ij} = 1$ if the end of the tube at node i is filled with a wetting fluid, and the end at node j is filled with a nonwetting fluid, $s = -1$ otherwise.

Since $M_{ij} = M_{ji}$, and $s_{ij} = -s_{ji}$ we have

$$A_{ij} = A_{ji}, \tag{9}$$

$$B_{ij} = -B_{ji}. \tag{10}$$

The average fluid velocity in the capillary τ_{ij} is

$$v_{ij} = \frac{Q_{ij}}{\pi R_{ij}^2}. \tag{11}$$

The law of conservation of volume at the nodes for a closed system (in the absence of sources/sinks at the nodes) leads to a system of n linear equations for determining the pressures at the nodes:

$$\sum_j Q_{ij} = 0, \quad i = 1, 2, \ldots, n, \tag{12}$$

where j are the indexes of the nodes connected to node v_i. For example, in Fig. 1, $i = 3$, and $j = (1, 2, 4, 5)$. Taking equation (6) into account, we have

$$\sum_j A_{ij}(P_i - P_j) = -\sum_j B_{ij}, \quad i = 1, 2, \ldots, n. \tag{13}$$

In the problem of counter-current imbibition, we have a closed system, that is, no fluid can enter or leave the system. The determinant of the matrix of the system of linear equations is equal to zero (the summation of equations (13), due to (9) and (10) leads to the identity $0 = 0$). This case is solved by adding a constant to the elements of an arbitrary column k of the matrix of the linear equations, which enforces the additional condition $P_k = 0$.

The coordinates of the menisci, if present in the τ_{ij} tube, satisfy the equation

$$\frac{dx_{ij}}{dt} = v_{ij}. \tag{14}$$

Let us formulate the equations in dimensionless form by introducing the linear scale L_m, the pressure scale P_m and the dynamic viscosity scale μ_m, such that: $x = L_m\widetilde{x}$, $R_{ij} = L_m\widetilde{R}_{ij}$, $l_{ij} = L_m\widetilde{l}_{ij}$, $t = t_m\widetilde{t}$, $v_{ij} = v_m\widetilde{v}_{ij}$, $P = P_m\widetilde{P}$, $M_{ij} = \mu_m\widetilde{M}_{ij}$. We define:

$$v_m \equiv \frac{L_m P_m}{\mu_m}, \quad t_m \equiv \frac{L_m}{v_m}. \tag{15}$$

The flow equations in dimensionless form are

$$\frac{d\widetilde{x}_{ij}}{d\widetilde{t}} = \widetilde{v}_{ij}, \tag{16}$$

$$\widetilde{v}_{ij} = \frac{\widetilde{R}_{ij}^2}{8\widetilde{M}_{ij}\widetilde{l}_{ij}}\left(\Delta\widetilde{P}_{ij} + \frac{1}{N}\frac{2s_{ij}}{\widetilde{R}_{ij}}\right), \tag{17}$$

where N is the capillary number, which is a dimensionless parameter characterizing the relationship between the viscous and the capillary forces:

$$N = \frac{v_m \mu_m}{\sigma} = \frac{L_m P_m}{\sigma}. \tag{18}$$

Note that the capillary number N can be expressed in terms of the radius R_{ref} and the length l_{ref} of the tube, with a pressure difference at the ends of the capillary of scale P_m:

$$\widetilde{v}_{ij} = \frac{\widetilde{R}_{ij}^2}{8\widetilde{M}_{ij}\widetilde{l}_{ij}}\left(\Delta\widetilde{P}_{ij} + \frac{\alpha}{N_c}\frac{2s_{ij}}{\widetilde{R}_{ij}}\right), \tag{19}$$

$$N_c \equiv \frac{R_{\text{ref}}^2 P_m}{8 l_{\text{ref}} \sigma}, \quad \alpha = \frac{N_c}{N} = \frac{R_{\text{ref}}^2}{8 l_{\text{ref}} L_m}. \tag{20}$$

In the problem of capillary imbibition we choose the value $P_m = \frac{\sigma}{R_{\text{ref}}}$ as the pressure scale and $L_m = R_{\text{ref}}$ as the length scale, then $N = 1$ and equations (16) and (17) take dimensional form. The distribution of wetting and nonwetting fluids along the outgoing flows at each node is determined from the condition of minimum contact energy of the nonwetting fluid with the walls of the capillaries, the implementation of which in a network model is the novelty. A brief version of the algorithm:

1. Calculation of pressure at all nodes for the given configuration of menisci by solving the system of linear equations (13).

2. Determination of the time integration step Δt, such that $\Delta t = \frac{c_t l}{v_{\max}}$, here $v_{\max}$ is the maximum velocity among all tubes, for all results in this article we have used $c_t = 0.1$.

3. Integration of equation (14) per time step Δt to calculate the displacements of menisci and the volumetric inflow and outflow in each node v_k.

4. Distribution of fluids in each node v_k according to the novel method, which is the wetting fluid is first distributed into the tubes according to the ascending order of their radii, and then the non-wetting fluid.

5. Recalculation of the position of the meniscus (merging of drops) when more than 2 menisci appear in a tube, such that the center of mass of each fluid in the tube remains the same.

In what follows all quantities are dimensionless, so the sign "~" is omitted.

3. Imbibition of an inclusion at a constant saturation

Using the developed algorithm, we solve the problem of imbibition of an inclusion inside a region with closed boundaries. Initially, the wetting fluid is located in the outer region and the nonwetting fluid is located in the inner region as shown in Fig. 2, *a*. During simulation, we calculate the saturation of the wetting fluid $S(t)$ in the inner region and the average capillary pressure P_c in the inner region were for various equilibrium values of S.

The computational domain consists of a grid of 30×30 tubes. The tubes in the outer region have radii of $R_{\text{outer}} = 6$. The inner region (inclusion) consists of thinner tubes with radii consisting of $R_{\text{inner}} = (2, 3, 4, 5)$. The volume of the inner region is approximately equal to the volume of the outer region, $V_{\text{inner}} \approx V_{\text{outer}}$, where $V_{\text{sys}} = V_{\text{inner}} + V_{\text{outer}}$.

Random small values are added to the initial radii of the tubes R_{ij}^0 that is $R_{ij} = R_{ij}^0 + \Delta R_{ij}$, thus preventing the case of two identical tubes being connected to a node, and thus ensuring that there

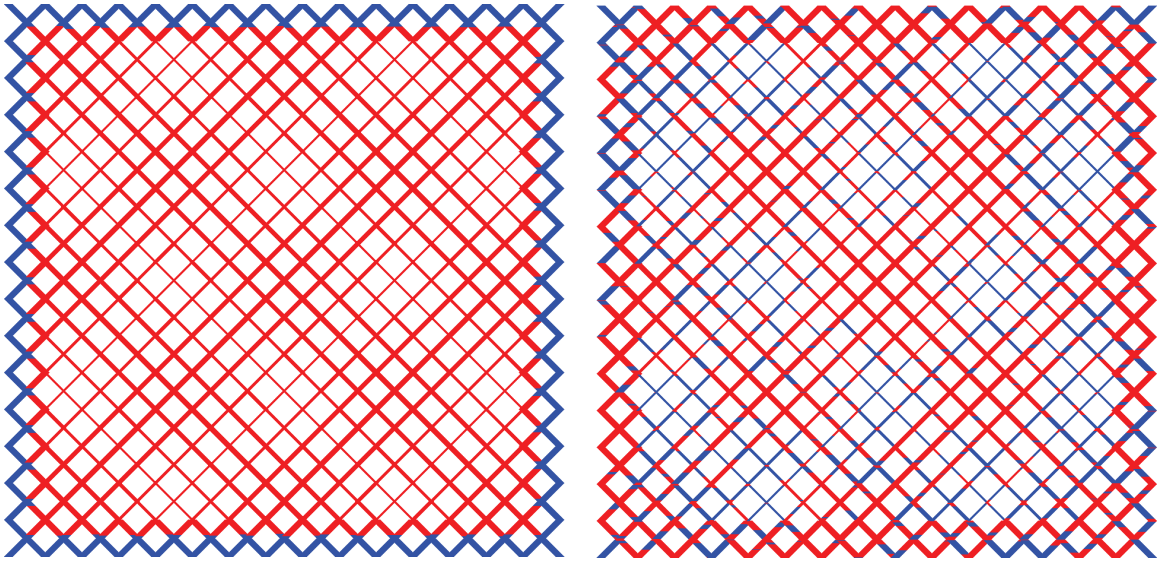

(a) $S_{sys} = 0.29$, $S_{inner} = 0$ (b) $S_{sys} = 0.29$, $S_{inner} = 0.30$

Figure 2. Flow visualization for counter-current imbibition, in 30×30 grid of tubes. S_{sys} is saturation of wetting fluid in the whole system, which remains constant, S_{inner} is saturation of wetting fluid in the inner region. All boundaries are closed. (a) Initial distribution, where the inner region of low-permeability is saturated with nonwetting, and outer region of high-permeabality with wetting fluid. The wetting fluid invades the inner region solely due the capillary forces. (b) Final distribution, wetting fluid prefers to rest in the thinner capillaries

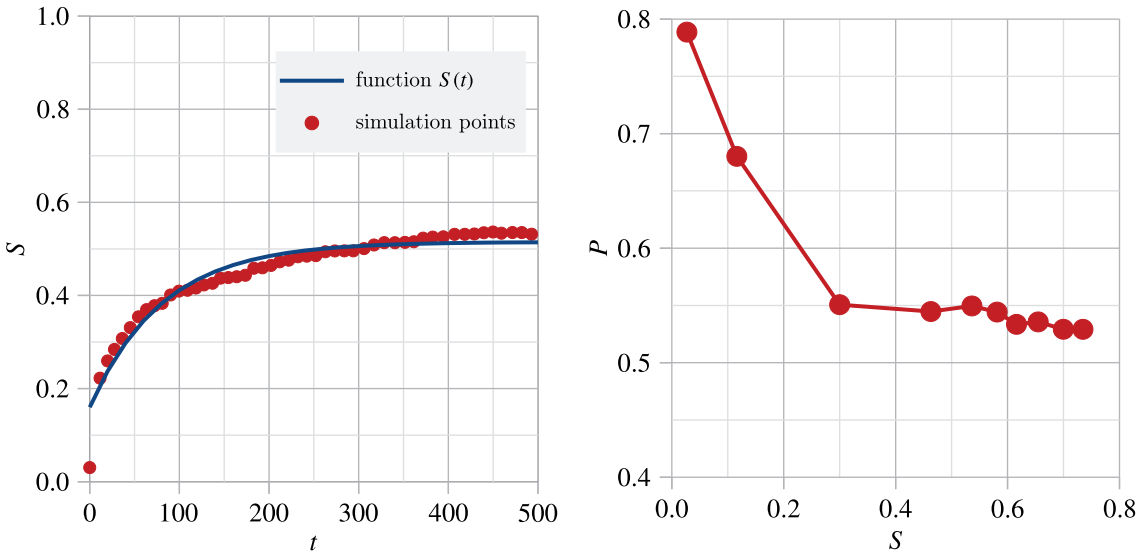

(a) Saturation vs time (b) Capillary pressure vs saturation

Figure 3. Results for counter-current imbibition. (a) Dependence of saturation S of the wetting fluid in the inner region with respect to dimensionless time t. (b) The dependence of average capillary pressure P (dimensionless) with respect to equilibrium saturation S

always exists a unique way of distributing fluids according to the novel method. In all results shown here, $\frac{\Delta R_{ij}}{R^0_{ij}} \approx \pm 10^{-3}$. The other constants used were: $\mu_1 = \mu_2 = 0.05$, $\sigma = 1$ and $l = 20$.

Series of calculations were carried out for different saturations of the wetting fluid in the whole system S_{sys}, where a system consists of the inner and the outer region. An example of the initial and

equilibrium configuration of fluids in a tube system is shown in Fig. 3. It can be seen that the wetting fluid preferentially penetrates the tubes of smaller radius.

Figure 3, *a* shows an example of the evolution of the saturation of the wetting fluid in the inner region over time for the case of maximum saturation 0.53. The calculated curve can be approximated quite well using the function

$$S(t) = C_1 + C_2\left(1 - e^{-C_3 t}\right), \tag{21}$$

where C_1, C_2 and C_3 are fitting coefficients. In Fig. 3, *b*, we see that the average capillary pressure decreases with increase in equilibrium saturation, this is in agreement with the well-known theory and experimental results [Fatt, 1956].

4. Flow in a periodically inhomogeneous medium

Let us consider the process of displacement of a nonwetting fluid by a wetting fluid in a periodically inhomogeneous porous medium. Heterogeneity is modeled by varying the radii of the tubes. The radius of a tube is a function of the coordinate of its center (shown in Fig. 4, *a*):

$$R(x, y) = A(1 + B\cos(k_x x)\cos(k_y y)), \tag{22}$$

where $A = 4$, $B = 0.8$, $k_x = k_y = \frac{2\pi}{\lambda}$, $\lambda = 10\delta$, δ is the distance between two adjacent nodes, $\delta = \sqrt{2}l$, and l is the length of the tube.

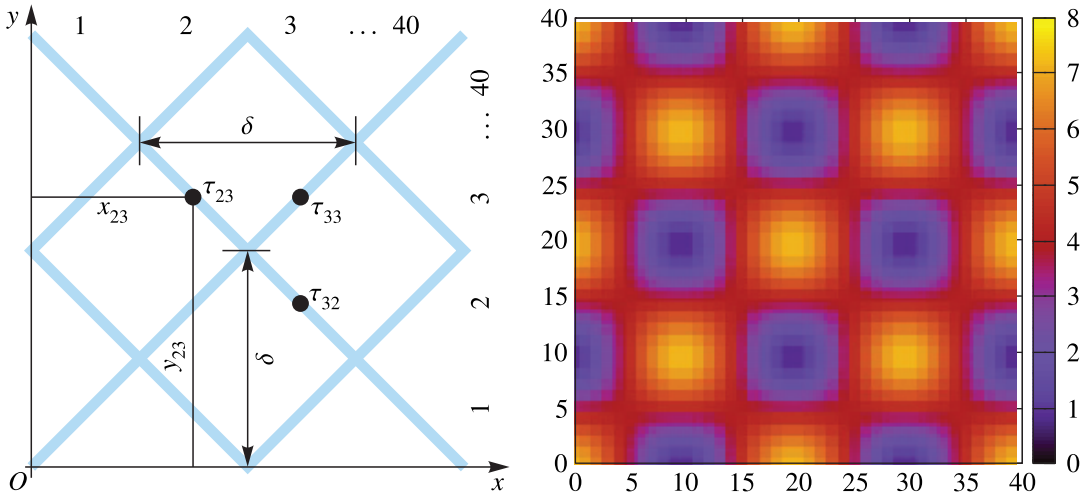

(a) Dimensions (b) Thickness of radii

Figure 4. Radius distribution for filtration. (a) Simplified view of 40×40 tubes, with marked centers of 3 tubes τ_{32}, τ_{33}, and τ_{23}. The center of τ_{23} located at (x_{23}, y_{23}). δ is the distance between any two adjacent nodes along an axis. (b) Periodical nonhomogeneity, heat map of radius distribution produced by equation (22), the numbers along the horizontal and vertical axes denote the kth row and column of the grid formed by tubes

The setup and boundary conditions are shown in Fig. 5. The top and bottom rows of nodes are closed boundaries, while the left and right column of nodes are open boundaries. The wetting fluid is injected at a constant flow rate Q from the left. All open nodes on the left boundary are maintained at the same input pressure $P_{\text{in}}(t)$, which are calculated at each computation step, in order to achieve $Q =$ $=$ const for various different distributions of menisci. Fluids are drained from the right open nodes, which is always maintained at a pressure $P_{\text{out}} =$ const. We terminate the simulation when we have

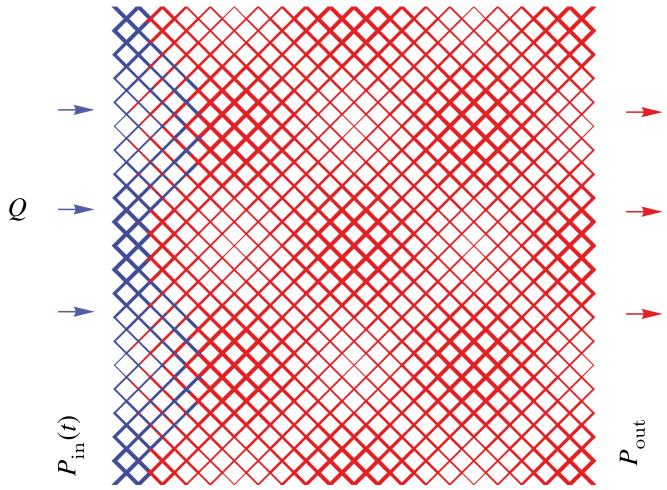

Figure 5. Boundary conditions for filtration. 40×40 tubes, $N = 1$, $t = 1000$, where N is the capillary number according to equation (18), and t is time in dimensionless form. Q is the volumetric injection rate, $P_{in}(t)$ is the input pressure, and P_{out} is the output pressure, all quantities are in dimensionless form

injected the wetting fluid of volume approximately equal to the total volume of the system V_{sys}. The physical time t_{max} for the simulation is

$$\int_0^{t_{max}} Q\,dt = V_{sys}; \tag{23}$$

since $Q = \text{const}$, we have

$$t_{max} = \frac{V_{sys}}{Q}, \tag{24}$$

where $V_{sys} = \sum\limits_i \pi R_i^2 l$ for all tubes i.

For all results of filtration we have used: a grid of size 40×40 tubes; $\mu_1 = \mu_2 = 0.01$; $l = 100$; $P_{out} = 10.0$; $Q = 1000$. We calculate $V_{sys} = 9.7 \cdot 10^6 \approx 10^7$, and therefore from equation (24), $t_{max} \approx \frac{10^7}{10^3} = 10^4$.

We see flow visualization for the high capillary number $N = 1$ and the low capillary number for $N = 0.05$ in Fig. 6 and Fig. 7, respectively. In Fig. 6, it is clear that the fluid prefers to flow through the path of least resistance, which are the thicker tubes. In Fig. 6, *a*, the flow (front) is the least progressed along the horizontal axis of symmetry as the region there has thinner capillaries. In Fig. 6, *b*, we see formation of zones with nonwetting fluid located in the intersection of the thinner capillaries temporarily surrounded by the wetting fluid on all its sides. In Fig. 7, the wetting fluid prefers to flow through the thinner tubes with higher capillary forces. In Fig. 7, *a*, the flow through the thinner tubes has moved the furthest ahead, partially surrounding the zones of intersection of the thicker tubes. In Fig. 7, *b*, we see the formation of zones with the nonwetting fluid located in the intersection of the thicker capillaries temporarily surrounded by the wetting fluid on all its sides.

In Fig. 8 we see three positions of the saturation front at different times for $N = 1$. Saturation $S(x, t)$ was calculated from the volume fraction of the wetting fluid within a vertical strip of thickness $\frac{\delta}{2}$. In Fig. 9, we see a comparison of the positions of saturation fronts at the same time $t = 4000$ for different N. Oscillations in saturation graphs are associated with the heterogeneity of the medium. It can be seen that for lower capillary numbers the oscillations are stronger. This is due to the fact that the volume of tubes in the region with thin tubes is much less than the volume of tubes in the region with thicker tubes.

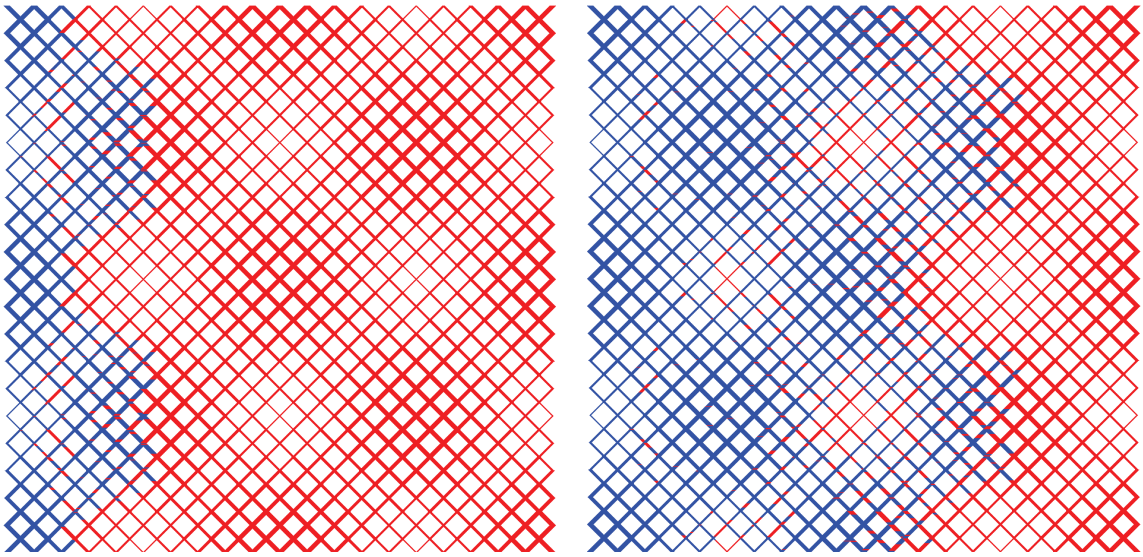

(a) $t = 2000$ (b) $t = 6000$

Figure 6. Flow visualization for filtration. 40×40 tubes, $N = 1$, high capillary number, corresponding to low capillary force, at various t, where N is the capillary number according to equation (18), and t is time in dimensionless form

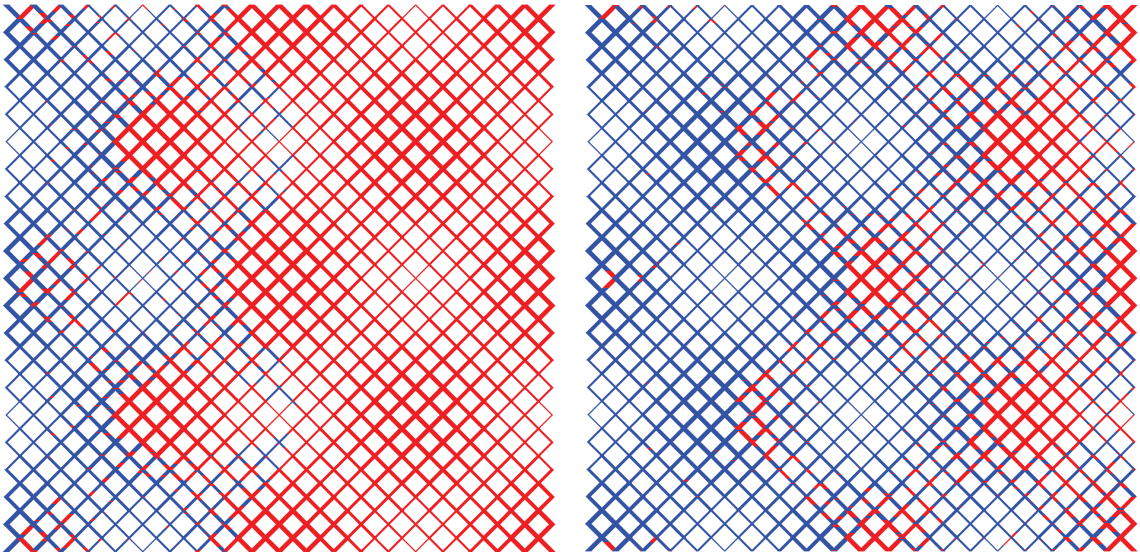

(a) $t = 2000$ (b) $t = 6000$

Figure 7. Visualization of flow for filtration in inhomogeneous porous medium. 40×40 tubes, $N = 0.05$, low capillary number, corresponding to high capillary force, at various t, where N is the capillary number according to equation (18), and t is time in dimensionless form

5. Conclusion

We developed a network model which uses a novel method of distributing phases at the nodes. We proposed two test problems: the problem of counter-current imbibition in an inclusion, and the problem of displacement in a periodically inhomogeneous porous media. We have observed the following properties: capillary imbibition, dependence of capillary pressure on saturation, the effect of capillary forces in two-phase displacement, which are analogous in real porous media. In the second

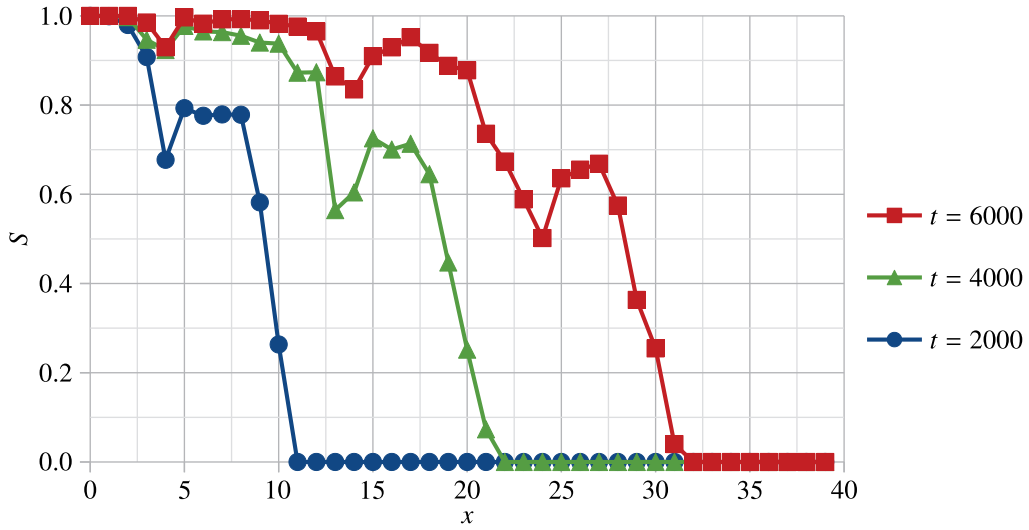

Figure 8. Results for filtration in inhomogeneous porous medium. 40×40 tubes, $N = 1$. S versus coordinate x for various t. Here, N is the capillary number according to equation (18), and t is time in dimensionless form. $S = S(x, t)$ is the saturation of the wetting fluid in the column of tubes located at x, where x is the number of tubes along the horizontal from the origin O, about O and x shown in detail in Fig. 4, *a*

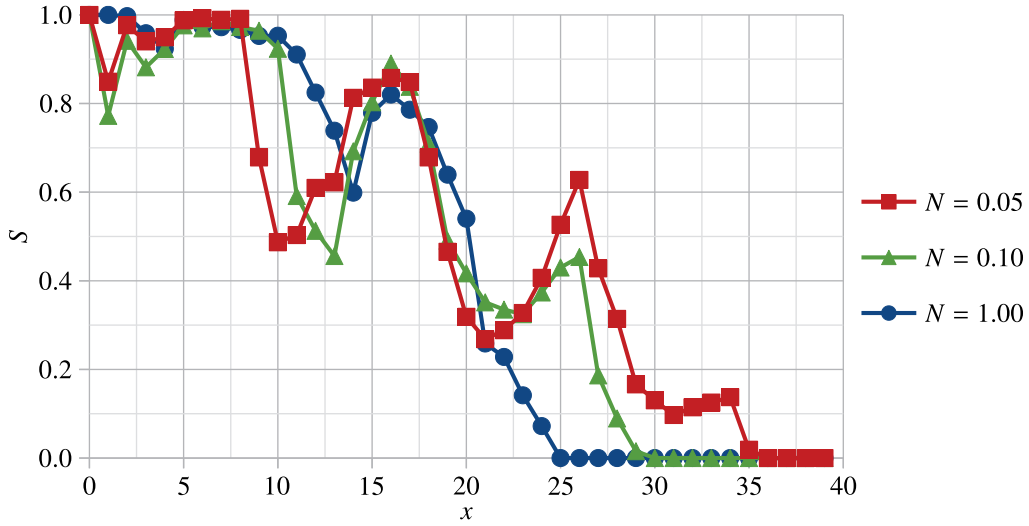

Figure 9. Results for filtration in inhomogeneous porous medium. 40×40 tubes, at $t = 4000$. S versus coordinate x for various N. Here, N is the capillary number according to equation (18), and t is time in dimensionless form. $S = S(x, t)$ is the saturation of the wetting fluid in the column of tubes located at x, where x is the number of tubes along the horizontal from the origin O, about O and x shown in detail in Fig. 4, *a*

problem about filtration in a periodically inhomogeneous porous medium, the result shows that, for higher value of capillary number, the wetting fluid prefers to invade through the thicker tubes, which is the path of the least resistance and in the case of lower, through thinner tubes. It is clear that at low capillary numbers the fluid predominantly moves through thin capillaries. At low capillary numbers the redistribution of fluids in the pore space occurs faster than at high capillary numbers. Thus, the flow with small capillary numbers is closer to the equilibrium case. Most importantly, the method of distributing fluids in a node is valid and can be extended to an arbitrary number of connections, which will be used in developing a network model for three dimensions. For the dependence of average capillary pressure vs saturation in the problem of counter-current imbibition, a qualitative agreement

with known experimental and theoretical results has been obtained. This will further allow the network model to be used to verify other homogenized models of capillary nonequilibrium.

6. Appendix

The source code used is located here: https://github.com/kafiulshabbir/porus-fluid.

References

Aker E. et al. A two-dimensional network simulator for two-phase flow in porous media // Transport in porous media. — 1998. — Vol. 32. — P. 163–186.

Barenblatt G., Patzek T., Silin D. The mathematical model of nonequilibrium effects in water – oil displacement // SPE journal. — 2003. — Vol. 8, No. 4. — P. 409–416.

Barenblatt G., Zheltov I., Kochina I. Basic concepts in the theory of seepage of homogeneous liquids in fissured rocks // Journal of applied mathematics and mechanics. Pergamon. — 1960. — Vol. 24, No. 5. — P. 1286–1303.

Blunt M. et al. Pore-scale imaging and modelling // Advances in Water resources. Elsevier. — 2013. — Vol. 51. — P. 197–216.

Chen S., Doolen G. Lattice Boltzmann method for fluid flows // Annual review of fluid mechanics. — 1998. — Vol. 30, No. 1. — P. 329–364.

Coussy O. Poromechanics. — John Wiley & Sons, 2004. — P. 315.

Fatt I. The network model of porous media. 3. Dynamic properties of networks with tube radius distribution // Transactions of the American institute of mining and metallurgical engineers. — 1956. — Vol. 207, No. 7. — P. 164–181.

Hassanizadeh S. Continuum description of thermodynamic processes in porous media: Fundamentals and applications // Modeling Coupled Phenomena in Saturated Porous Materials. — 2004. — P. 179–223.

Hassanizadeh S., Gray W. High velocity flow in porous media // Transport in porous media. Springer. — 1987. — Vol. 2. — P. 521–531.

Kondaurov V. I. A non-equilibrium model of a porous medium saturated with immiscible fluids // Journal of Applied Mathematics and Mechanics. Elsevier. — 2009. — Vol. 73, No. 1. — P. 88–102.

Kondaurov V. I. The thermodynamically consistent equations of a thermoelastic saturated porous medium // Journal of applied mathematics and mechanics. Elsevier. — 2007. — Vol. 71, No. 4. — P. 562–579.

Konyukhov A., Pankratov L., Voloshin A. Homogenized non-equilibrium models of two-phase flow in fractured porous media. — Moscow: Fizmatkniga, 2017. — P. 187.

Konyukhov A., Pankratov L., Voloshin A. The homogenized Kondaurov type non-equilibrium model of two-phase flow in multiscale non-homogeneous media // Physica Scripta. — 2019. — Vol. 94, No. 4.

Labed N., Bennamoun L., Fohr J. Experimental study of two-phase flow in porous media with measurement of relative permeability // Fluid Dyn. Mater. Process. Citeseer. — 2012. — Vol. 8, No. 4. — P. 423–436.

Liu J., Lin L., Song R., Zhao J. A pore scale modeling of fluid flow in porous medium based on Navier – Stokes equation // Disaster Advances. — 2013. — Vol. 6. — P. 5–11.

Meakin P., Tartakovsky A. Modeling and simulation of pore-scale multiphase fluid flow and reactive transport in fractured and porous media // Reviews of Geophysics. Wiley Online Library. — 2009. — Vol. 47, No. 3.

Ramstad T., Berg C., Thompson K. Pore-scale simulations of single- and two-phase flow in porous media: approaches and applications // Transport in Porous Media. Springer. — 2019. — Vol. 130. — P. 77–104.

Shabbir K. Simulation of two-phase flow in porous media using a two-dimensional network model // Proceedings of the 65th all Russia Scientific Conference MIPT. — Moscow: Fizmatkniga. — 2023. — Vol. 78. — P. 205–206.

Su B., Sanchez C., Yang X. Insights into hierarchically structured porous materials: from nanoscience to catalysis, separation, optics, energy, and life science // Hierarchically Structured Porous Materials. Wiley Online Library. — 2012. — P. 1–27.

Whitaker S. Flow in porous media. I: A theoretical derivation of Darcy's law // Transport in porous media. — 1986. — Vol. 1. — P. 3–25.